Carrier transport processes in dye sensitized solar cells based on Zn_2SnO_4 nanostructures studied by intensity modulated photocurrent/photovoltage spectroscopy

Jiajun Chen and Wenyong Wang[a)]
Department of Physics & Astronomy, University of Wyoming, Laramie, Wyoming 82071, USA

(Received 6 April 2013; accepted 14 May 2013; published online 31 May 2013)

In this work, the electron transport and recombination processes in dye sensitized solar cells (DSSCs) based on Zn_2SnO_4 nanowires and nanoparticles were studied by intensity modulated photocurrent spectroscopy (IMPS)/photovoltage spectroscopy. Two distinct transport time constants were obtained from the IMPS spectra of Zn_2SnO_4 nanowire-DSSCs, which were associated with a fast, direct transport through the single crystalline structure of the nanowires and a slow, percolation transport that was assisted by the nanowire surface states, respectively. The charge collection efficiency for the fast transport process was close to unity in all the measurements at different light intensities, indicating that the overall charge collection efficiency of nanowire-DSSCs could be enhanced if the slow transport process could be suppressed. © *2013 AIP Publishing LLC*.
[http://dx.doi.org/10.1063/1.4808344]

Due to the advantages such as low fabrication cost and flexible device structure, dye sensitized solar cells (DSSCs) have attracted significant research interests since the groundbreaking work of O'Regan and Grätzel.[1] Typical photoanode materials in DSSCs are binary metal oxides such as TiO_2 that has produced the best power conversion efficiency thus far.[2,3] However, studies have also shown that TiO_2 can create photobleaching problems for the dye molecules, suggesting the need to search for other suitable photoanode materials.[4,5] Zn_2SnO_4 is a wide bandgap ternary metal oxide with a conduction band edge similar to that of TiO_2 but has a higher electron mobility ($\sim 10\,cm^2/V \cdot s$).[6,7] Recently, Zn_2SnO_4 nanoparticles (NPs) and nanowires (NWs) have been utilized in DSSCs as the photoanodes, and promising device performance has been reported.[8–10] On the other hand, many experimental methods have been developed to characterize carrier transport and recombination processes in photoanode materials.[11,12] Among them, Intensity Modulated Photocurrent/Photovoltage Spectroscopy (IMPS/VS) and Transient Photocurrent/Photovoltage decay (TPC/TPV) measurements are widely used ones, and IMPS/VS can especially provide a better understanding of the complex charge transport processes in DSSCs. For instance, the charge generation profile can be studied by examining the shapes of the semicircles in IMPS spectra,[13] and the effect of the electrolyte on carrier transport can also be inspected,[14,15] which are typically difficult to achieve with TPC/TPV measurements. However, thus far, there are only limited publications on IMPS/VS studies of DSSCs based on single crystalline metal oxide nanowires,[16,17] and there are no such reports on Zn_2SnO_4 nanowire-DSSCs. In our previous study, we have investigated the synthesis of Zn_2SnO_4 nanowires and their photovoltaic applications,[10,18] and in this work, we continued to use the IMPS/VS characterization method to study the charge transport and recombination processes in DSSCs based on Zn_2SnO_4 nanostructures.

The device structures of DSSCs based on Zn_2SnO_4 nanowires and nanoparticles are shown in Figures 1(a) and 1(b), respectively. The synthesis of Zn_2SnO_4 nanowires and fabrication of DSSCs followed the procedures reported elsewhere.[10] The Zn_2SnO_4 nanowires were grown on silicon substrates by chemical vapor deposition, and the lengths of the nanowires were $\sim 200\,\mu m$ and the diameters were $\sim 80\,nm$. After growth, the nanowires were transferred to fluorine-doped-tin-oxide (FTO) coated glass substrate using a stamping method. The Zn_2SnO_4 nanoparticles were prepared following the published procedure,[8] and were applied onto the FTO substrate by the doctor-blade method followed by annealing at 500 °C in air. The thicknesses of the Zn_2SnO_4 nanowire and nanoparticle films were both $20\,\mu m$. For dye loading, the photoanode thin films were soaked in 0.05 mM

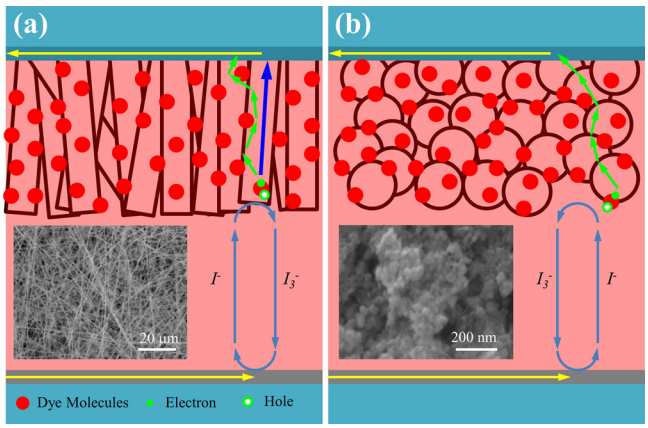

FIG. 1. (a) Schematic showing the structure of a Zn_2SnO_4 nanowire-DSSC. The blue and green lines indicate the fast and slow electron transport processes in the nanowire-photoanode, respectively. (b) Schematic showing the structure of a Zn_2SnO_4 nanoparticle-DSSC. The green line indicates the electron transport process in the nanoparticle-photoanode. The insets are SEM images of Zn_2SnO_4 nanowires and nanoparticles, respectively.

[a)]Author to whom correspondence should be addressed. Email address: wwang5@uwyo.edu

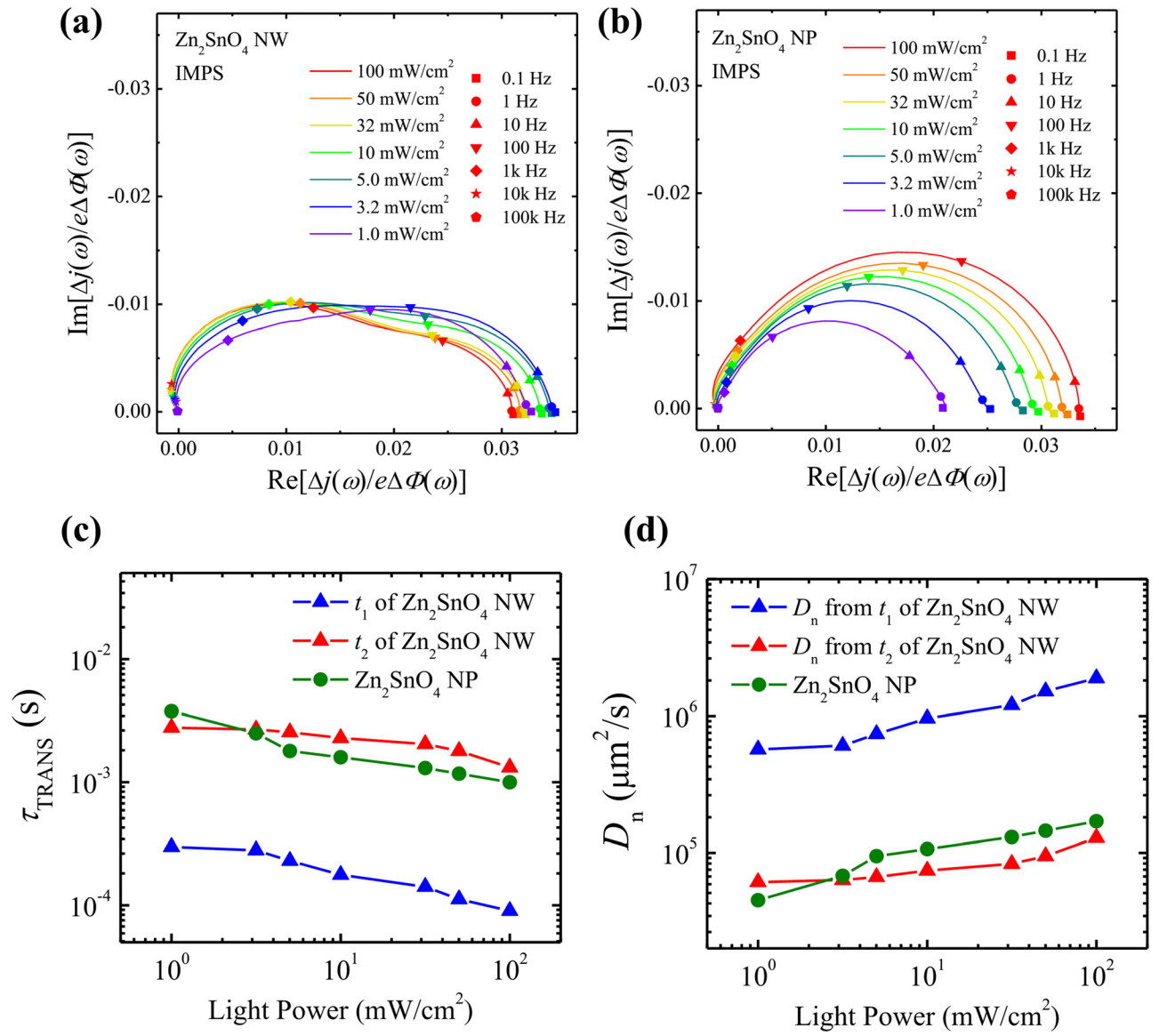

FIG. 2. IMPS spectra of DSSCs based on (a) Zn_2SnO_4 NWs and (b) Zn_2SnO_4 NPs. (c) Electron transport time constants obtained from the IMPS spectra at different white light intensities. (d) Electron diffusion coefficients calculated from the transport time constants at different light intensities.

N719 dye ethanol solution for 24 h. FTO substrate coated with 20 nm Pt was used as the counter electrode, and the liquid electrolyte was a mixture of 50 mM I_2, 0.5 M LiI, and 0.5M 4-tertbutylpyridine in 3-methoxypropionitrile.

For IMPS/VS measurements, a white light emitting diode (LED) array driven by a Yokogawa 7651 low-noise DC power supply was used to provide the constant background illumination. A red light ($\lambda = 625$ nm) LED ring was used to provide the sinusoidal optical perturbation signal, whose intensity was modulated by the output of a Stanford SR780 dynamic signal analyzer. The transfer function module of SR780 was used to detect the IMPS/VS signals, and before entering SR780 the photocurrent response from the DSSCs was amplified by a Stanford SR570 current preamplifier. The intensity of the modulation light was kept less than 10% of the white light intensity in all of measurements. The obtained IMPS/VS spectra were fitted using Eq. (1) for one time constant or Eq. (2) for two time constants with a nonlinear-least-squares fitting program developed under the Levenberg-Marquardt algorithm[19,20]

$$\begin{aligned} \mathrm{Re[IMPS\ or\ IMVS]} &= \frac{M_1}{1+(\omega\tau)^2}, \\ \mathrm{Im[IMPS\ or\ IMVS]} &= -\frac{M_2\omega\tau}{1+(\omega\tau)^2}, \end{aligned} \tag{1}$$

$$\begin{aligned} \mathrm{Re[IMPS\ or\ IMVS]} &= \frac{M_1}{1+(\omega\tau_1)^2} + \frac{M_2}{1+(\omega\tau_2)^2}, \\ \mathrm{Im[IMPS\ or\ IMVS]} &= -\frac{M_3\omega\tau_1}{1+(\omega\tau_1)^2} - \frac{M_4\omega\tau_2}{1+(\omega\tau_2)^2}, \end{aligned} \tag{2}$$

where M_1, M_2, M_3, M_4, τ, τ_1, and τ_2 are the fitting parameters. For a single time constant process, M_1 is the low-frequency limit of the real part, while for a two time constants process, $M_1 + M_2$ is the low-frequency limit. The electron transport time constant, τ_{TRANS}, and the recombination time constant, τ_{REC}, can be obtained from the fitting of the IMPS and IMVS spectra, respectively.

Figures 2(a) and 2(b) show the Nyquist plots of IMPS data of Zn_2SnO_4 nanowire- and nanoparticle-DSSCs,

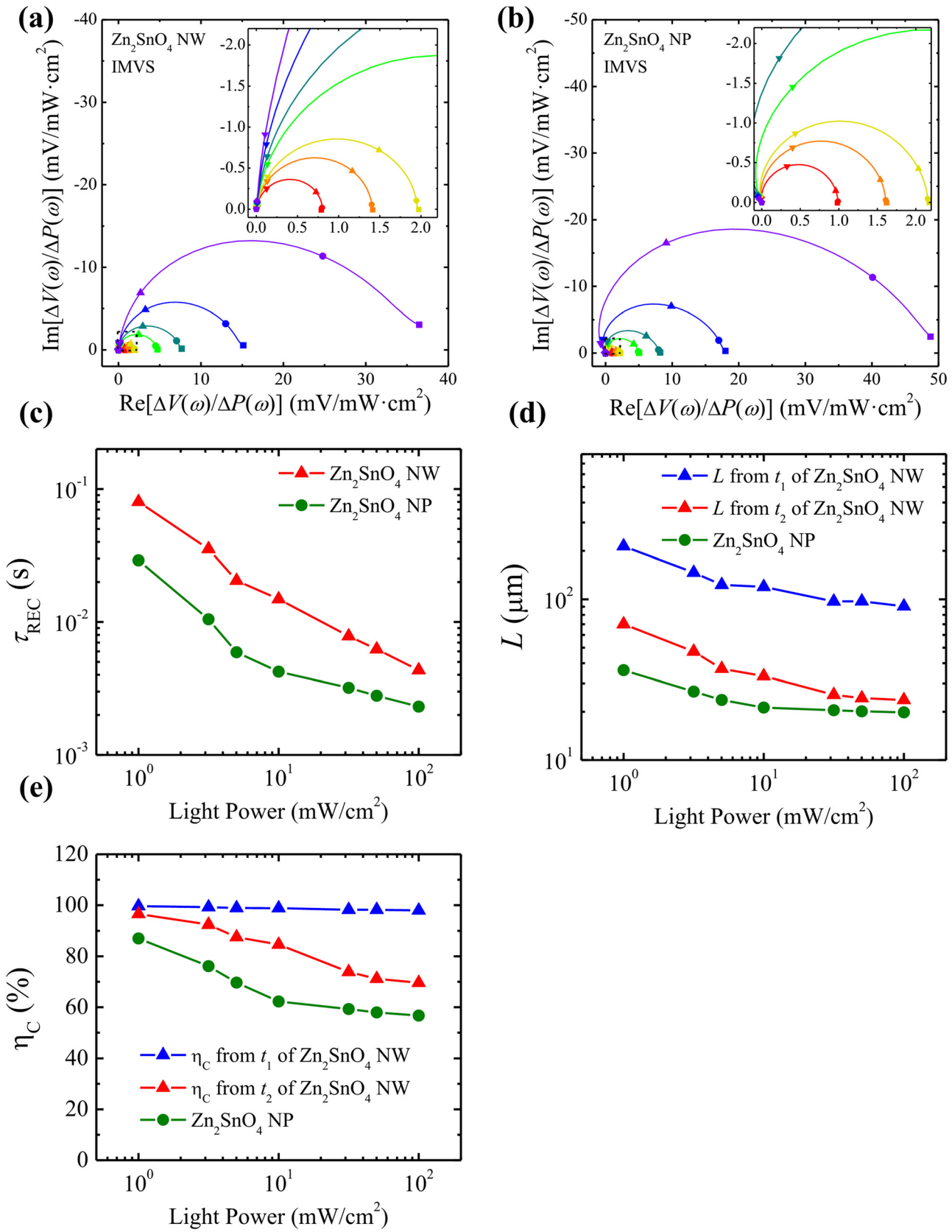

FIG. 3. IMVS spectra of DSSCs based on (a) Zn_2SnO_4 nanowires and (b) Zn_2SnO_4 nanoparticles. The insets are enlarged plots of the squared areas. (c) Electron recombination time constants obtained from the IMVS spectra at different white light intensities. (d) Electron diffusion lengths calculated from the diffusion coefficients and recombination time constants. (e) Charge collection efficiencies of the Zn_2SnO_4 nanowire- and nanoparticle-DSSCs at different light intensities.

respectively, obtained at different light intensities in the frequency range of 0.1 Hz to 100 kHz. From these plots, it can be seen that the electron transport in Zn_2SnO_4 nanowire-photoanodes was very different from that in the nanoparticle-photoanodes. The IMPS spectra of the nanowire-photoanodes exhibited two merged semicircles, while the spectra of the nanoparticle-photoanodes only showed one semicircle. Two semicircles in IMPS spectra of

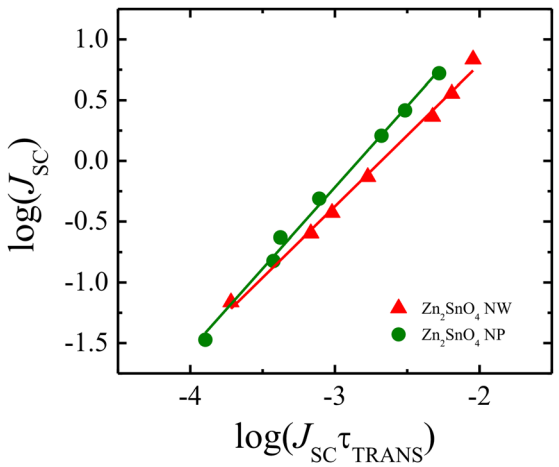

FIG. 4. Double logarithmic plots to get the average trap depth of the Zn_2SnO_4 photoanodes. The symbols represent the data obtained at different light intensities, and the lines are linear fittings.

nanoparticle-photoanodes have been reported before, which is attributed to two different electron transport processes in the photoanodes due to an exponential carrier generation profile.[13,21–23] In this interpretation, the semicircle at high frequency corresponds to a direct charge diffusion transport towards the collection electrode, while the semicircle at low frequency corresponds to the charge diffusion in the opposite direction and reflected back afterwards by the edge of the photoanode.[13] However, this is unlikely the case observed in this study. First, a blue light was used as the modulation in the previous research, which has a high absorption coefficient and can indeed produce an exponential carrier generation profile in the nanoparticle-photoanodes.[21,23] In our study, however, a red light ($\lambda = 625$ nm) was used as the modulation, and hence a near-uniform carrier generation in the photoanodes was expected.[11,19] Second, in this study, the two semicircles were only observed in the spectra of the Zn_2SnO_4 nanowire-photoanodes, but not in the spectra of the nanoparticle-photoanodes, which is different from the aforementioned situation. Therefore, the two semicircles observed here must relate to carrier transport processes in the Zn_2SnO_4 nanowire-photoanodes that were different from those suggested in the previous theory.

Using Eqs. (1) and (2) nonlinear-least-squares fittings of the IMPS spectra were carried out to obtain the transport time constants, and Figure 2(c) shows the fitting results. The two time constants extracted from the IMPS spectra of Zn_2SnO_4 nanowire-photoanodes were labeled as t_1 and t_2 in Figure 2(c), which corresponded to a fast and a slow transport process, respectively. τ_{TRANS} obtained from the IMPS spectra of Zn_2SnO_4 nanoparticle-photoanodes is also shown in the sample figure. From this figure, it can be seen that the time constant of the slow transport process in the nanowire-photoanodes was very close to the transport time constant of the nanoparticle-photoanodes, while the time constant of the fast process in the nanowires was almost one order of magnitude faster than the above two. Therefore, we suggest that the slow transport in the Zn_2SnO_4 nanowire-photoanodes was dominated by a surface trap state-assisted percolation process, just as what happens in a typical nanoparticle-photoanode, while the fast transport was a direct diffusion conduction through the crystalline structure of the Zn_2SnO_4 nanowires (see illustrations in Figure 1). The electron diffusion coefficient D_n can be estimated using the transport time constant and $D_n = \frac{w^2}{2.35\tau_{TRANS}}$, where w is the thickness of the photoanode film.[24] The calculated electron diffusion coefficients associated with the above three time constants are plotted in Figure 2(d), and the diffusion coefficient of the fast transport process in Zn_2SnO_4 nanowires was consequently one order of magnitude larger than the other two, which was as high as 1.8×10^6 $\mu m^2/s$ at 1 Sun. Several transport measurements of Zn_2SnO_4 nanowire field effect transistors reported electron mobility values close to 10 $cm^2/V \cdot s$.[7] Using the Einstein relation, $\frac{D_n}{\mu} = \frac{kT}{e}$, where μ is the electron mobility, k is the Boltzmann constant, T is the temperature, and e is the elementary charge, the electron diffusion coefficient can be calculated using the mobility measurement result. The estimated D_n of Zn_2SnO_4 nanowires from the transistor transport measurements is $\sim 10^7$ $\mu m^2/s$, which is closer to the D_n value of the fast transport process obtained from the IMPS measurement, indicating that the fast transport was likely associated with the direct transport in the single crystalline Zn_2SnO_4 nanowire structure. However, more studies that involve the examination of the effects of the dye molecules and electrolyte on the nanowire surface states are needed in order to fully characterize and understand the fast and slow transport processes observed here. Another observation from Figure 2(c) is that all the transport time constants slightly decreased when the white light intensity was increased, which could be attributed to the influence of a higher level surface trap state filling under the increased illumination intensity, as discussed in previous publications.[21–23,25]

Figures 3(a) and 3(b) show the IMVS measurement results of Zn_2SnO_4 nanowire- and nanoparticle-DSSCs, respectively, which were obtained in the same light intensity and frequency ranges as those used for the IMPS measurements. Unlike the IMPS spectra, all of the IMVS spectra exhibited single semicircles, from which the electron recombination time constants could be derived. The obtained recombination time constants of the Zn_2SnO_4 nanowire- and nanoparticle-DSSCs are plotted in Figure 3(c). It can be seen that the recombination time constant of the nanowire-DSSCs was constantly higher than that of the nanoparticle-DSSCs at different light intensities, which could be partially attributed to the smaller surface area of the nanowire-photoanodes that suppressed the back electron transfer reaction at the photoanode/electrolyte interface. Such an effect has been discussed in previous publications, which was also related to an improved open-circuit voltage.[10,26] The recombination time constants of both types of DSSCs also decreased monotonically when the light intensity was increased, which could be explained by an enhancement in the recombination rate constant through surface states when the quasi-Fermi level moved toward the conduction band due to the increased light intensity.[27] From the diffusion coefficient and recombination time constant, the charge diffusion length can be calculated using $L = \sqrt{D_n \tau_{REC}}$,[24] and the obtained results of Zn_2SnO_4 nanowire- and nanoparticle-DSSCs are shown in Figure 3(d). The diffusion length of the fast transport process in the nanowires was 2–3 times longer than that of the slow

process. Although the slow process in the Zn_2SnO_4 nanowires had a similar diffusion coefficient as that of the Zn_2SnO_4 nanoparticles, the diffusion length of the slow process was still longer due to the larger electron recombination time constant of the nanowire-DSSCs. A key parameter to evaluate the performance of DSSCs is the charge collection efficiency η_{CC} that can be determined by the transport and recombination time constants using $\eta_{CC} = 1 - \frac{\tau_{TRANS}}{\tau_{REC}}$. The electron collection efficiencies of the Zn_2SnO_4 nanowire- and nanoparticle-DSSCs studied in this work are plotted in Figure 3(e). It can be seen that the fast transport process in the Zn_2SnO_4 nanowires produced an electron collection efficiency that was close to 100% even at 1 Sun, while the slow process showed a collection efficiency of ~65% under the same condition, but was still higher than that of the nanoparticle-DSSCs. This observation suggested that the overall electron collection efficiency of nanowire-DSSCs could be enhanced if proper surface passivation methods could be developed to suppress the slow transport process in the nanowire-photoanodes.

Another information that can be derived from IMPS/VS measurements is the energy depth that the trap states can extend into the bandgap of the metal oxide photoanodes. For carrier transport process, the trap states can be either surface states or bulk defect states, but for the recombination process only the surface trap states are involved.[28] The density of trap states is generally described by an exponential distribution that is extended from the conduction band edge into the bandgap of the photoanode: $g(E) = g_0 \exp\left(\frac{E-E_C}{m_C}\right)$, where E is the energy of the trap state, E_C is the conduction band edge, g_0 is a constant, and m_C represents the average trap depth.[21,28–30] Using $g(E)$, the trapping and detrapping rate constants of the photo-generated electrons during the transport process can be determined.[21] The average trap depth m_C is the slope of the exponential trap distribution curve, which can be estimated from the slope of a double logarithmic plot of J_{SC} vs $J_{SC} \cdot \tau_{TRANS}$.[31] Figure 4 shows such plots for photoanodes based on Zn_2SnO_4 nanowires and nanoparticles, where the symbols represent the data obtained at different light intensities and the lines are linear fittings. From the slopes of the linear fittings, the m_C values of the Zn_2SnO_4 photoanodes could be estimated, which were in the range of 30–35 meV, representing the average energy depth that the trap states could extend into the Zn_2SnO_4 bandgap. These values were significantly smaller than that of the TiO_2 photoanodes, which is ~69 meV, indicating that the trap states in Zn_2SnO_4 were more concentrated near the conduction band edge than the trap states in TiO_2 do.[31]

In summary, the electron transport and recombination processes in Zn_2SnO_4 nanowire- and nanoparticle-photoanodes were studied by IMPS and IMVS in this work. The IMPS measurements of Zn_2SnO_4 nanowire-photoanodes yielded two distinct transport time constants, which were interpreted as representing a fast, direct transport through the single crystalline structure of the nanowires and a slow, percolation transport that was mediated by the nanowire surface states, respectively. Evaluation of the cell charge collection efficiency suggested that the overall electron collection efficiency of nanowire-DSSCs could be enhanced if suitable passivation approaches could be developed to suppress the slow transport process in the nanowire-photoanodes.

This work was supported by the U.S. Department of Energy, Office of Basic Energy Sciences, Division of Materials Sciences and Engineering under Award No. DE-FG02-10ER46728.

[1]B. O'Regan and M. Grätzel, Nature **353**, 737 (1991).
[2]M. Gratzel, Inorg. Chem. **44**, 6841 (2005).
[3]A. Yella, H.-W. Lee, H. N. Tsao, C. Yi, A. K. Chandiran, M. K. Nazeeruddin, E. W.-G. Diau, C.-Y. Yeh, S. M. Zakeeruddin, and M. Gratzel, Science **334**, 629 (2011).
[4]M. Muruganandham and M. Swaminathan, Sol. Energy Mater. Sol. Cells **81**, 439 (2004).
[5]G. A. Epling and C. Lin, Chemosphere **46**, 561 (2002).
[6]M. A. Alpuche-Aviles and Y. Wu, J. Am. Chem. Soc. **131**, 3216 (2009).
[7]C. Pang, B. Yan, L. Liao, B. Liu, Z. Zheng, T. Wu, H. Sun, and T. Yu, Nanotechnology **21**, 465706 (2010).
[8]B. Tan, E. Toman, Y. Li, and Y. Wu, J. Am. Chem. Soc. **129**, 4162 (2007).
[9]T. Lana-Villarreal, G. Boschloo, and A. Hagfeldt, J. Phys. Chem. C **111**, 5549 (2007).
[10]J. Chen, L. Lu, and W. Wang, J. Phys. Chem. C **116**, 10841 (2012).
[11]H. Wang and L. M. Peter, J. Phys. Chem. C **113**, 18125 (2009).
[12]H. K. Dunn and L. M. Peter, J. Phys. Chem. C **113**, 4726 (2009).
[13]J. Halme, K. Miettunen, and P. Lund, J. Phys. Chem. C **112**, 20491 (2008).
[14]H. Wang, P. G. Nicholson, L. Peter, S. M. Zakeeruddin, and M. Grätzel, J. Phys. Chem. C **114**, 14300 (2010).
[15]J. J. Nelson, T. J. Amick, and C. M. Elliott, J. Phys. Chem. C **112**, 18255 (2008).
[16]E. Enache-Pommer, B. Liu, and E. S. Aydil, Phys. Chem. Chem. Phys. **11**, 9648 (2009).
[17]A. B. F. Martinson, J. E. McGarrah, M. O. K. Parpia, and J. T. Hupp, Phys. Chem. Chem. Phys. **8**, 4655 (2006).
[18]Q. Dai, J. Chen, L. Lu, J. Tang, and W. Wang, Nano Lett. **12**, 4187 (2012).
[19]G. Schlichthörl, S. Y. Huang, J. Sprague, and A. J. Frank, J. Phys. Chem. B **101**, 8141 (1997).
[20]G. Schlichthörl, N. G. Park, and A. J. Frank, J. Phys. Chem. B **103**, 782 (1999).
[21]A. C. Fisher, L. M. Peter, E. A. Ponomarev, A. B. Walker, and K. G. U. Wijayantha, J. Phys. Chem. B **104**, 949 (2000).
[22]F. Cao, G. Oskam, G. J. Meyer, and P. C. Searson, J. Phys. Chem. **100**, 17021 (1996).
[23]L. Dloczik, O. Ileperuma, I. Lauermann, L. M. Peter, E. A. Ponomarev, G. Redmond, N. J. Shaw, and I. Uhlendorf, J. Phys. Chem. B **101**, 10281 (1997).
[24]J. van de Lagemaat and A. J. Frank, J. Phys. Chem. B **105**, 11194 (2001).
[25]L. Peter and K. Wijayantha, Electrochim. Acta **45**, 4543 (2000).
[26]S. Y. Huang, G. Schlichthörl, A. J. Nozik, M. Gratzel, and A. J. Frank, J. Phys. Chem. B **101**, 2576 (1997).
[27]M. D. Archer and A. J. Nozik, *Nanostructured and Photoelectrochemical Systems for Solar Photon Conversion* (Imperial College Press, London, 2008).
[28]J. Bisquert, F. Fabregat-Santiago, I. Mora-Seró, G. Garcia-Belmonte, and S. Giménez, J. Phys. Chem. C **113**, 17278 (2009).
[29]J. M. Marshall, Rep. Prog. Phys. **46**, 1235 (1983).
[30]A. J. Frank, N. Kopidakis, and J. van de Lagemaat, Coord. Chem. Rev. **248**, 1165 (2004).
[31]J. van de Lagemaat and A. J. Frank, J. Phys. Chem. B **104**, 4292 (2000).